lncRNA Ttc3-209 Promotes the Apoptosis of Retinal Ganglion Cells in Retinal Ischemia Reperfusion Injury by Targeting the miR-484/Wnt8a Axis

Ran Zhang,[1,2] Yuqing Feng,[1,2] Jinfang Lu,[1,2] Yanni Ge,[1,2] and Huiling Li[1,2]

[1]Department of Ophthalmology, The Second Xiangya Hospital, Central South University, Changsha, Hunan 410011, China
[2]Hunan Clinical Research Center of Ophthalmic Disease, Changsha, Hunan 410011, China

Correspondence: Huiling Li, Department of Ophthalmology, Second Xiangya Hospital, Central South University, Changsha, Hunan 410011, China; lihuiling@csu.edu.cn.

Received: December 13, 2020
Accepted: February 25, 2021
Published: March 9, 2021

Citation: Zhang R, Feng Y, Lu J, Ge Y, Li H. lncRNA Ttc3-209 promotes the apoptosis of retinal ganglion cells in retinal ischemia reperfusion injury by targeting the miR-484/Wnt8a axis. *Invest Ophthalmol Vis Sci.* 2021;62(3):13. https://doi.org/10.1167/iovs.62.3.13

Purpose. Apoptosis of the retinal ganglion cells (RGCs) can cause irreversible damage to visual function after retinal ischemia reperfusion injury (RIR). Using a lncRNA chip assay, we selected lncRNA Ttc-209 and characterized its role in RGCs during ischemia reperfusion (I/R)–induced apoptosis.

Methods. We created an ischemic model of RGCs by applying Hank's balanced salt solution containing 10 µM antimycin A and 2 µM calcium ionophore for 2 hours. RIR was induced in mice by elevating the intraocular pressure to 120 mm Hg for 1 hour by cannulation of the cornea; this was followed by reperfusion. Real-time quantitative PCR was used to detect the expression levels of long noncoding RNA (lncRNA), microRNA (miRNA), and target gene mRNA. Western blotting, flow cytometry, immunofluorescent staining, and TUNEL assays were performed to detect cell apoptosis. Dual-luciferase reporter assays and FISH were used to identify endogenous competitive RNA (ceRNA) mechanisms that link lncRNAs, miRNAs, and target genes. We also used scotopic electroretinography examinations to evaluate visual function in treated mice.

Results. lncRNA Ttc3-209 was significantly upregulated after I/R injury and played a proapoptotic role in RGCs during I/R-induced apoptosis. Mechanistically, lncRNA Ttc3-209 is a ceRNA that competitively binds to miR-484 and upregulates the translation of its target (Wnt8a mRNA), thus promoting apoptosis in RGCs.

Conclusions. Reducing the expression of lncRNA Ttc3-209 had a protective effect against apoptosis in RGCs. This may provide a new therapeutic option for the prevention of RGC apoptosis in response to RIR injury.

Keywords: lncRNA Ttc3-209, miR-484, wnt8a, retinal ischemia reperfusion, RGCs, apoptosis

Retinal ischemia reperfusion (RIR) is a common pathophysiologic process that occurs during the development of various ophthalmic diseases, including glaucoma, diabetic retinopathy, and ischemic optic neuropathy; these diseases represent a serious threat to human vision.[1,2] Apoptosis of the retinal ganglion cells (RGCs) is a notable feature of retinal damage following ischemia reperfusion (I/R) and can be triggered by a variety of stimuli and a series of intrinsic and extrinsic pathways.[3,4] Over recent decades, several studies have investigated the molecular mechanisms of apoptosis in RGCs. A variety of molecules have been associated with this process, including proapoptotic kinases, the Bcl-2 family of proteins, mitochondrial dysfunction, caspases, the p53 tumor suppressor, TNFα, the Fas ligand, and Fas/CD95.[4] However, the precise regulatory factors that control the apoptotic process in RGC apoptosis have yet to be fully elucidated.

Long noncoding RNAs (lncRNAs) are nonprotein coding transcripts made up of more than 200 nucleotides.[5,6] Numerous studies have demonstrated that lncRNAs play a vital role in different cellular processes, such as proliferation, differentiation, migration, invasion, and apoptosis, and exhibit differential expression in the pathogenesis of ophthalmologic disorders.[5,7–12] Interestingly, some studies have suggested that the lncRNA-mRNA competitive endogenous RNA network plays a role in the transcriptional regulation of I/R injury, in which lncRNA functions as a competitive endogenous RNA (ceRNA) that competes for microRNA (miRNA) in order to increase the expression of a particular target gene.[13–16] Therefore, we hypothesized whether lncRNAs could influence the process of apoptosis in RGCs via the ceRNA pathway in a mouse model of I/R damage.

In our previous studies, we unexpectedly found that the lncRNA ENSMUST00000139607 (lncRNA Ttc3-209) was upregulated when we induced I/R damage in RGCs via a lncRNA chip assay.[17] lncRNA Ttc3-209 is located on chromosome 16: 94,440,093-94,448,745 (forward strand); the biological functions of this lncRNA and its correlations with disease have not been reported previously. miR-484 is known to suppress the translation of mitochondrial fission protein Fis1 and inhibit Fis1-mediated fission and apoptosis in cardiomyocytes and in adrenocortical cancer cells.[18]

The mRNA levels of wingless-related MMTV integration site 8A (Wnt8a), along with Wnt4b and Wnt11, are known to be significantly increased following the induction of apoptosis; data also showed that Wnt8a is produced in apoptotic cells in a caspase-dependent manner.[19] In the present study, we found that lncRNA Ttc3-209 acts as a ceRNA that competes for miR-484 and acts as a sponge for miR-484 in order to enhance the expression levels of Wnt8a, thus aggravating I/R-induced apoptosis in RGCs. In addition, we also replicated the regulatory mechanisms created by the lncRNA Ttc3-209/miR-484/Wnt8a axis in C57BL/6J mice.

Materials and Methods

Antibodies and Reagents

Caspase-3 (cat. 9662) and cleaved caspase-3 (cat. 9661) were purchased from Cell Signaling Technology (Danvers, MA, USA). Wnt8a (cat. PA5-103481) was acquired from Invitrogen (Carlsbad, CA, USA). β-Tubulin (cat. 10094-1-AP) was obtained from Proteintech North America (Rosemont, IL, USA). Goat Anti-Rabbit IgG (H + L) HRP (cat. S0001) and Goat Anti-Mouse IgG (H + L) HRP (cat. S0002) were purchased from Affinity Biosciences (Cincinnati, OH, USA). We also acquired a FITC Annexin V Apoptosis Detection Kit I (cat. 556547) and PE Annexin V Apoptosis Detection Kit I (cat. 559763) from BD Pharmingen (San Diego, CA, USA) and a FISH kit (cat. C10910) was obtained from Ribobio (Guangzhou, Guangdong Province, China). We also acquired a dual-luciferase reporter assay system kit (cat. E1910) from Promega (Madison, WI, USA).

Cell Culture and Treatments

The cells used in this project were primary mouse RGCs and were isolated from the retinas of suckling mice (1–4 days postnatal). All procedures were carried out according to previously described methods but with minor modifications.[20,21] Under a sterile environment, we first coated a 24-well plate with poly-D-lysine (P6407; Sigma, St. Louis, MO, USA) and laminin (L-6274; Sigma). We also used purified donkey anti-rabbit IgG (H + L) to coat 75-cm^2 cell culture flasks for antimacrophage panning. Rabbit anti-rat IgG (H + L) was used to coat a 100-cm^2 dish for a Thy1.2 antibody. These were incubated overnight at 4°C. Next, 5 mL Dulbecco's Phosphate Buffered Saline (DPBS), containing 30 µL Thy1.2 antibody (BE0066; Bio X Cell, West Lebanon, NH, USA), was added to the 100-cm^2 dish. The retinas were washed in DPBS using a pipette and then transferred to papain solution for incubation at 37°C for 15 minutes. Low ovomucoid was added to the cells with rabbit anti-mouse microphage antibody (AIA31240; Accurate Chemical, Westbury, NY, USA) and incubated at room temperature for 5 minutes. The high ovomucoid was washed and panning buffer was added to increase the volume. Next, we transferred the cell suspension to the antimacrophage flask prepared previously and incubated this at room temperature for 40 minutes. The cell suspension was then filtered through a Nixtex (Sefar America Inc., Depew, NY, USA) mesh and transferred to a Thy1.2 dish for 1 hour. Next, 4 mL trypsin/Earle's Balanced Salt Solution (EBSS) was added to digest the RGCs off the dish; the reaction was then terminated after 5 minutes. Next, the cells were pelleted by centrifugation at 200 × g for 5 minutes and then resuspended in preequilibrated RGC whole growth medium. Laminin was then removed from the poly-D-lysine that coated the culture plates. The cell suspension was then plated and the RGCs were cultured in a moist atmosphere with 5% CO_2 and 95% O_2 at 37°C; 50% of the media was replaced with prewarmed whole growth medium every 3 days.

An ischemic model of RGCs was established using methods that were described previously.[22] When the RGCs had covered over 90% of the plate, the medium was changed to Hank's balanced salt solution containing 10 µM antimycin A (ab141904; Abcam, Cambridge, MA, USA) and 2 µM calcium ionophore (A2318; Aladdin, Shanghai, China) dissolved in dimethylsulfoxide (DMSO) for 2 hours. The whole growth medium was then harvested and sustained for 0, 1, 2, and 4 hours.

For gene knockdown and overexpression experiments, we used Lipofectamine 2000 to transfect the RGCs with lncRNA Ttc3-209 siRNA, lncRNA Ttc3-209 plasmid, miR-484 mimic, miR-484 inhibitor, Wnt8a siRNA, and scramble siRNA (Ribobio); the transfections were carried out in accordance with the manufacturer's instructions. When the density of the RGCs on the 24-well plate reached 80% to 90%, we added the preprepared 50-nM transfection solution to the cell culture dish. After 6 hours, the transfection solution was removed and replaced with whole growth medium.

Real-Time Quantitative PCR

Total RNA was extracted from the RGCs and retinas of C57BL/6J mice using Trizol Reagent (Invitrogen, Carlsbad, CA, USA) in accordance with the manufacturer's protocol. Next, 40 ng total RNA was reverse-transcribed into cDNA via the use of a Prime Script RT Reagent Kit and a gDNA Eraser Kit (RR047A; TaKaRa, Tokyo, Japan). To detect the expression levels of lncRNA, miRNA, and target gene mRNA, we used real-time quantitative PCR (qPCR) and SYBR Green (K0221; ThermoFisher Scientific, Waltham, MA, USA). We then calculated ΔCt values via the application of StepOne Software (Applied Biosystems, Carlsbad, CA, USA). The sequences for lncRNA Ttc3-209 and miR-484 were retrieved from the GenBank database (gene IDs: 22129 and 723916, respectively); the primer sequences are described in the Supplementary Data.

Western Blotting

Proteins were obtained from RGCs and the retinas of mice. Following cell lysis, lysates underwent ultrasonic homogenization and centrifugation and were then denatured by boiling. Protein concentrations were then measured by a NanoDrop 2000 Spectrophotometer (ThermoFisher Scientific, Waltham MA, USA). Equal amounts (30 µg) of proteins were then loaded into each well and separated by 10% or 12% SDS-PAGE. Separated proteins were then transferred onto polyvinylidene difluoride membranes. The blots were then probed with primary antibodies against caspase-3 (1:1000), cleaved caspase-3 (1:1000), Wnt8a (1:2000), and β-tubulin (1:1000). This was followed by incubation with appropriate secondary antibodies (Goat Anti-Rabbit IgG (H + L) HRP [1:5000] or Goat Anti-Mouse IgG (H + L) HRP [1:5000]). Positive antibody binding was visualized by enhanced chemiluminescence (WBKLSO500; Millipore, Merck KGaA, Darmstadt, Germany) and a Tanon-5200Multi system (Tanon, Shanghai, China). Target protein bands were

Investigative Ophthalmology & Visual Science

then quantified by ImageJ software (National Institutes of Health, Bethesda, MD, USA), and β-tubulin was used as an internal control to normalize the expression levels.

Flow Cytometry Analysis of Apoptosis

RGCs were separated by 0.25% trypsin, washed twice with cold PBS, and then resuspended in 1× binding buffer at a concentration of 1×10^6 cells/mL. Next, 100 µL of this solution was transferred into a 5-mL culture tube, and 5 µL FITC Annexin V (or PE Annexin V) and 5 µL PI (or 7AAD) were added. The cells were gently vortexed and incubated for 15 minutes at room temperature in the dark. Finally, 400 µL of 1× binding buffer was added to the tube. Flow cytometry was then conducted within 1 hour with a BD FACSCalibur Flow Cytometer (San Diego, CA, USA). Data were analyzed by FlowJo V10 software (BD, San Diego, CA, USA).

FISH

RGCs were soaked in paraformaldehyde and hybridization buffer overnight at 37°C with lncRNA Ttc3-209, miR-484, and 18S rRNA (cytoplasm positive) fluorescence probes; these probes were synthesized by Ribobio. Cell nuclei were stained with DAPI. Fluorescence images were then captured by laser-scanning confocal microscopy (TCS SP5; Leica, Wetzlar, Germany).

Dual-Luciferase Reporter Assays

Dual-luciferase reporters (firefly luciferase and double-labeled *Renilla* luciferase) of lncRNA Ttc3-209 WT, lncRNA Ttc3-209 MUT, Wnt8a-WT, Wnt8a-MUT1, and Wnt8a-MUT2 were constructed and cotransfected with a miR-484 mimic or scramble. Cells were lysed by Passive Lysis Buffer 48 hours later. Then, Luciferase Assay Reagent II (LAR II) was added and firefly luciferase levels were detected. Next, Stop & Glo Reagent (Substrate + Buffer) and a ThermoFisher Varioskan LUX (Waltham, MA, USA) were used to detect *Renilla* luciferase levels. Firefly luciferase levels were normalized by the corresponding *Renilla* luciferase value. All plasmids were constructed by RuQi Biotechnology (Guangzhou, Guangdong Province, China).

Animal Models and Experimental Design

The animals used in this project were C57BL/6J mice; these were purchased from the Jackson Laboratory (Bach, Maine, USA). All experiments were carried out in accordance with the recommendations of the Institutional Committee for the Care and Use of Laboratory Animals of Second Xiangya Hospital, Central South University (China). Mice were housed under a 12-hour light/dark cycle and had free access to food and water. Experimental injuries were conducted under anesthesia by intraperitoneal injections of ketamine (100 mg/kg body weight; Ratiopharm Gmbh, Ulm, Germany) and xylazine (5 mg/kg; Bayer Vital Gmbh, Leverkusen, Germany). When the male C57BL/6J mice were 10 to 12 weeks old, they were preinjected directly into the binocular vitreous chamber (1 µL per injection, 1 µg/µL) with lncRNA Ttc3-209 siRNA or scramble.[23,24] Then, 24 hours after preinjection, I/R damage was applied. We selected the right eye as the "I/R" eye; intraocular pressure was elevated to 120 mm Hg for 1 hour by cannulation of the cornea to induce transient retinal ischemia; we then applied reperfusion of the eye for 24 hours, as described previously.[25,26] The contralateral eye was cannulated and maintained at normal intraocular pressure to serve as a control.[27,28] Eight mice from the same litter were used in pairs for real-time qPCR, immunofluorescence, TUNEL, and electroretinography (ERG). Mice used in the ERG test were sacrificed immediately after testing so that we could obtain retinas for Western blotting. Five independent replicates were carried out for each experiment.

Immunofluorescence and TUNEL Assays

After 24 hours of reperfusion, the eyes were removed and fixed in 4% paraformaldehyde for 1 hour. Following fixation, some of the retinas were removed for immunofluorescence staining. We also embedded whole eye cups in optimum cutting temperature compound and prepared 10-µm-thick cryosections with a freezing microtome. For immunofluorescence staining, the retinas were permeabilized and blocked in 10% Triton X-100 and 10% BSA for 1 hour. The sections were then incubated overnight with a primary antibody (Tuj1 [1:500], GB11139; Servicebio, Wuhan, Hubei Province, China) at 4°C. This was followed by a 2-hour incubation with a secondary antibody (Goat Anti-Rabbit IgG (H + L) Alexa Fluor 488 [1:1000], ab150077; Abcam) in the dark at room temperature (RT). The nuclei were then stained with DAPI. For TUNEL staining, frozen retinal sections were permeabilized and blocked in 0.1% Triton X-100 and 10% BSA for 1 hour. In accordance with the manufacturer's instructions (In Situ Cell Death Detection Kit TMR Red, 12156792910; Roche, Basel, Switzerland), a premixed enzyme solution (terminal deoxynucleotidyl transferase) containing label solution (TMR-dUTP) was incubated with the cryosections in the dark at 37°C for 1 hour. The nuclei were then stained with DAPI. Images were then captured by a Leica DMI3000B and analyzed by Photoshop software (Adobe, San Jose, CA, USA).

ERG

Previous research reported that a decline in b-wave amplitude represents a sensitive marker of retinal dysfunction after acute ocular ischemia.[29] We therefore used scotopic ERG examinations to evaluate the visual function of mice. After 6 hours of dark adaptation, the mice were given general anesthesia and placed on a test platform. The corneas were topically anesthetized with 4 mg/mL oxybuprocaine hydrochloride, and the pupils were dilated with 5 mg/mL compound tropicamide. Five electrodes were separately applied to the subcutaneous tissue of the tail and the cheeks, as well as the surface of the corneas. Flash ERG was recorded at an intensity of 3.0 cds/m^2. The system used for ERG was a Ganzfeld Q450 (ROLAND ELECTRONIC, Keltern, Germany), and data were analyzed by RETI-Port/Scan 21 software (ROLAND ELECTRONIC, Keltern, Germany).

Statistical Analysis

The two-tailed Student's *t*-test was used to compare differences between two groups. One-way ANOVA was performed for comparisons between multiple treatment groups. Two-way ANOVA was used to evaluate differences between multiple treatment groups at different time points. Data were expressed as the mean ± SD of five independent experiments. The results were statistically significant when

Investigative Ophthalmology & Visual Science

$P < 0.05$. All statistical analyses were performed with SPSS software and GraphPad Prism software (GraphPad Software, La Jolla, CA, USA).

Results

I/R Induced the Expression of lncRNA Ttc3-209 In Vitro and In Vivo

In our previous research, involving a lncRNA chip assay, we unexpectedly found that lncRNA Ttc3-209 was upregulated when we applied I/R damage to RGCs.[17] To verify this further, we established cell and animal models of ischemia and treated these with perfusion at specific time points. Real-time qPCR showed that under the same ischemic treatments, the expression levels of lncRNA Ttc3-209 in RGCs increased from 0 to 2 hours and peaked after 2 hours of reperfusion; levels then began to decline gradually (Fig. 1A). Consistently, the expression levels of lncRNA Ttc3-209 in the C57BL/6J mouse model, as determined by real-time qPCR, were all higher than the sham group and reached peak levels after 24 hours of reperfusion (Fig. 1B). To further confirm the expression levels of lncRNA Ttc3-209, we used a FISH assay to detect intracellular localization. Nuclei were stained by DAPI. 18S rRNA (cytoplasm-positive) and lncRNA Ttc3-209 were labeled with CY3. Results demonstrated that lncRNA Ttc3-209 was clearly localized in the cytoplasm of RGCs (Fig. 1C).

The Knockdown of lncRNA Ttc3-209 Attenuated I/R-Induced Apoptosis in RGCs

To clarify the function of lncRNA Ttc3-209 in RGCs during I/R-induced apoptosis, we first synthesized specific small interfering RNA (siRNA) against lncRNA Ttc3-209 and then assessed the efficiency of knockdown by real-time qPCR (Fig. 2A). In addition, Western blotting analysis showed that lncRNA Ttc3-209 siRNA significantly reduced the I/R-induced accumulation of cleaved caspase-3 in RGCs (Figs. 2B–D). Consistently, flow cytometry analysis of total cell apoptosis indicated that the I/R-induced apoptosis of RGCs was markedly inhibited by the transient gene silencing of lncRNA Ttc3-209 (Figs. 2E, 2F).

The Overexpression of lncRNA Ttc3-209 Aggravated I/R-Induced Apoptosis in RGCs

We cloned the full length of lncRNA Ttc3-209 into the pcDNA3.1 plasmid and then used real-time qPCR to analyze the efficiency of overexpression. Real-time qPCR showed that the I/R-induced expression of lncRNA Ttc3-209 could be further enhanced by the transfection of RGCs with the lncRNA Ttc3-209 plasmid (Fig. 3A). Moreover, Western blot analysis demonstrated that the overexpression of lncRNA Ttc3-209 significantly augmented the I/R-induced accumulation of cleaved caspase-3 in RGCs (Figs. 3B–D). Consistently, flow cytometry analysis of total cell apoptosis indicated that lncRNA Ttc3-209 overexpression also increased the I/R-induced apoptosis of RGCs (Figs. 3E, 3F).

miR-484 Was a Direct Target of lncRNA Ttc3-209

To determine the mechanism responsible for how lncRNA Ttc3-209 induces apoptosis in RGCs, we hypothesized that miRNAs may combine with lncRNA Ttc3-209 and used in silico analysis to screen the RegRNA database (http://regrna.mbc.nctu.edu.tw/index1.php). Finally, we selected miR-484 as the target that lncRNA Ttc3-209 binds to as a miRNA decoy. According to the predicted complementary sequence, we constructed dual-luciferase reporters for lncRNA Ttc3-209 WT and lncRNA Ttc3-209 MUT (Fig. 4A). Results indicated that luciferase activity was reduced after the cotransfection of RGCs with the lncRNA Ttc3-209 WT plasmid and the miR-484 mimic when compared with the negative control or the plasmid containing a mutated sequence of the presumptive binding site (Fig. 4B). Furthermore, the overexpression of lncRNA Ttc3-209 reduced the levels of miR-484, as detected by real-time qPCR. The knockdown of lncRNA Ttc3-209 exhibited the opposite effect (Figs. 4C, 4D). Furthermore, RNA FISH assays demonstrated that lncRNA Ttc3-209 and miR-484 both localized in the cytoplasm of RGCs and that the extent of this colocalization was elevated by I/R treatment (Fig. 4E).

The Overexpression of miR-484 Ameliorated I/R-Induced Apoptosis in RGCs

To understand the mechanism responsible for how lncRNA Ttc3-209 regulates apoptosis in RGCs, we first considered miR-484 as the point of penetration. Next, we transfected RGCs with miR-484 mimic or scramble with or without I/R damage. We then performed real-time qPCR to detect the expression levels of miR-484 (Fig. 5A). Next, we used Western blotting to test the changes in apoptosis-related protein expression and found that miR-484 protected RGCs against I/R-induced apoptosis (Figs. 5B, 5D). Flow cytometry analysis was then used to detect apoptosis in RGCs; data showed that the overexpression of miR-484 alleviated apoptosis in RGCs (Figs. 5E, 5F).

Wnt8a Was Identified as the Target Gene for miR-484

Further prediction of the target genes for miR-484 was performed by TargetScanMouse 7.2 (www.targetscan.org/mmu_72/); Wnt8a was eventually selected as the target gene for miR-484 with two putative binding sites in the 3′-UTR (Fig. 6A). After the transfection of RGCs with Wnt8a-WT, Wnt8a-MUT1, and Wnt8a-MUT2, we used dual-luciferase reporter assays to show that the cotransfection of the miR-484 mimic and the Wnt8a-WT plasmid significantly repressed luciferase activity when compared with the transfection of the negative control, Wnt8a-MUT1, or Wnt8a-MUT2 (Fig. 6B). We also transfected RGCs with the miR-484 mimic or scramble with or without I/R damage. Real-time qPCR demonstrated that the miR-484 mimic notably reduced both basal and I/R-induced mRNA levels of Wnt8a (Fig. 6C). Western blotting assays were also used to detect the protein expression levels of Wnt8; these assays confirmed the qPCR results (Figs. 6D, 6E).

The Knockdown of Wnt8a Suppressed I/R-Induced Apoptosis in RGCs

To identify the function of Wnt8a in I/R-treated RGCs, we transfected RGCs with Wnt8a siRNA or scramble with or without I/R damage. Wnt8a was induced by I/R treatment in RGCs at specific time points (Figs. 7A, 7B). Both Western

Investigative Ophthalmology & Visual Science

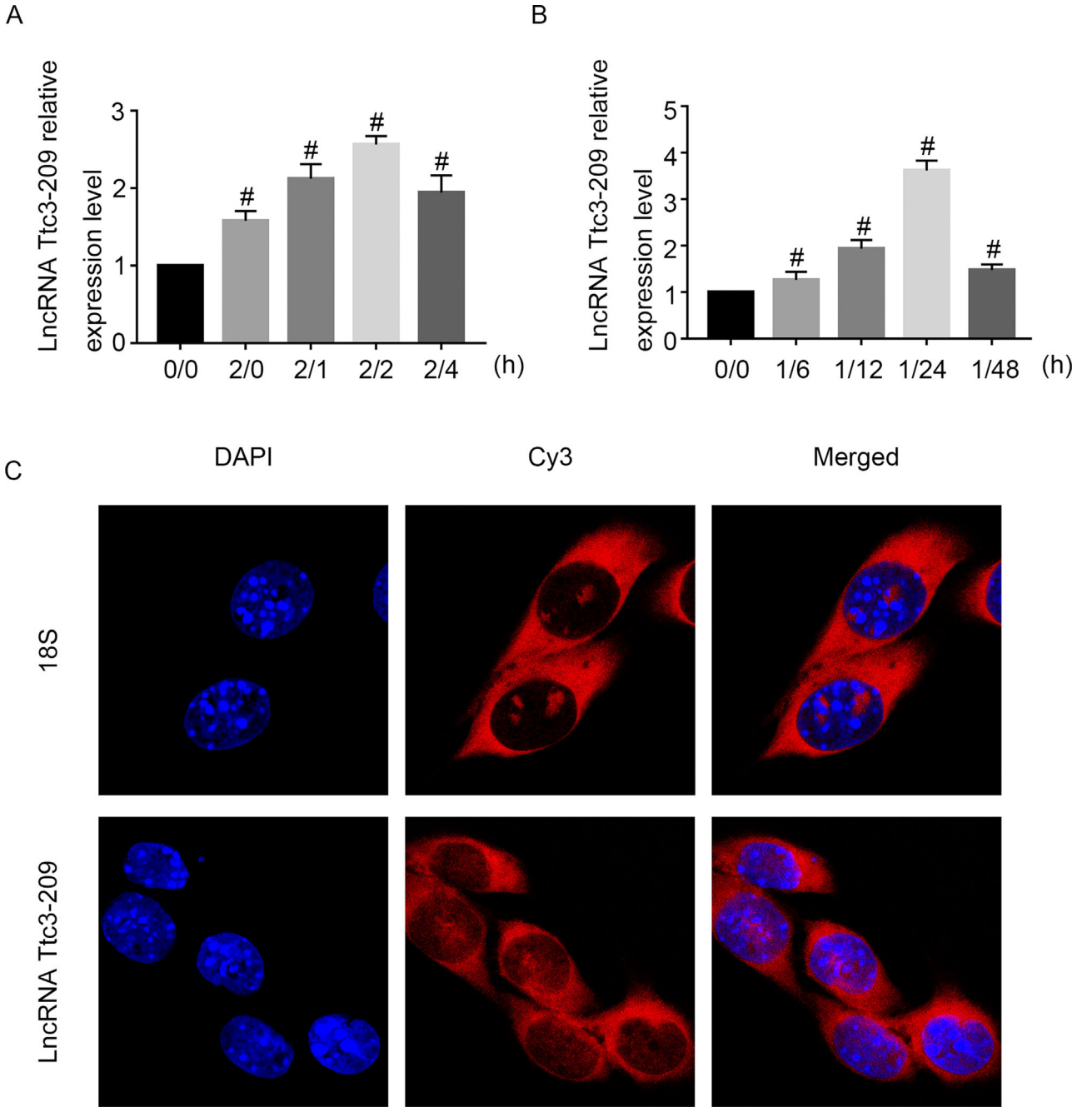

Figure 1. I/R induced the expression of lncRNA Ttc3-209 in vitro and in vivo. (**A**) Cultured primary mouse RGCs were treated with or without I/R damage at the indicated time points (I/R for 0/0, 2/0, 2/1, 2/2, 2/4 hours, respectively). The expression levels of lncRNA Ttc3-209 were detected by real-time qPCR. (**B**) The intraocular pressure was elevated to 120 mm Hg for 1 hour and then changed to reperfusion for 6, 12, 24, and 48 hours in C57BL/6J mice. The expression levels of lncRNA Ttc3-209 in the retinas were detected by real-time qPCR. (**C**) RNA FISH assays detected the intracellular localization of lncRNA Ttc3-209 in RGCs. *Scale bar*: 10 µm. Data are expressed as mean ± SD of five independent experiments; $^{\#}P < 0.05$ vs. 0/0 hour or sham group.

blotting and flow cytometry showed that the knockdown of Wnt8a reduced I/R-induced apoptosis in RGCs (Figs. 7C–H).

miR-484 Mediated the Proapoptotic Effects of lncRNA Ttc3-209

Next, we investigated whether miR-484 could mediate the proapoptotic effects of lncRNA Ttc3-209 in I/R-treated RGCs. Both lncRNA Ttc3-209 siRNA and miR-484 inhibitor were transfected into RGCs, and the transfection efficiency was validated by real-time qPCR (Figs. 8A, 8B). Western blotting analysis indicated that the downregulation of lncRNA Ttc3-209 alleviated the I/R-induced accumulation of cleaved caspase-3 and also suppressed the expression levels of Wnt8a; these effects were reversed by the miR-484 inhibitor (Figs. 8C–F). Flow cytometry analysis supported the Western

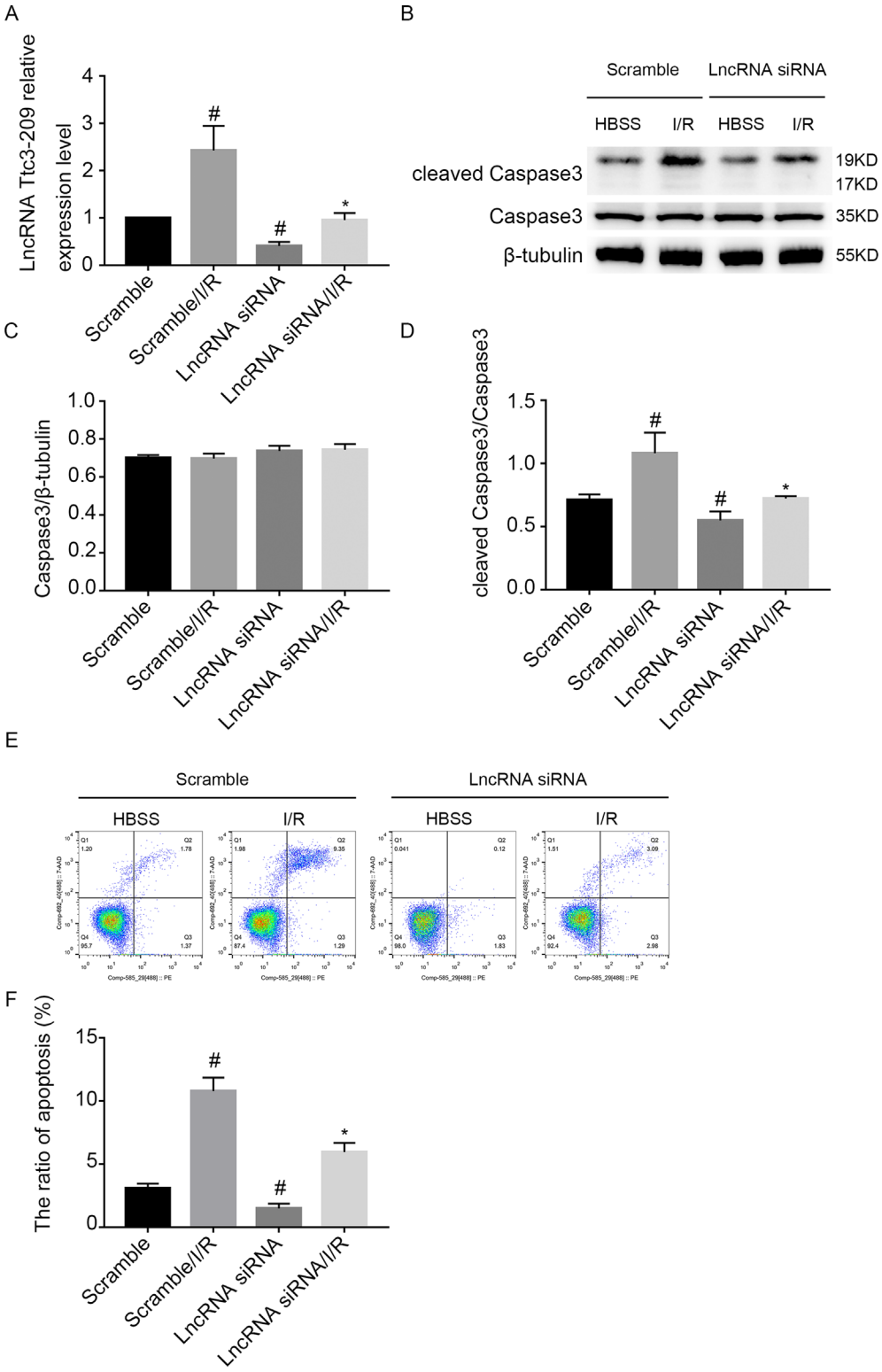

Figure 2. The knockdown of lncRNA Ttc3-209 attenuated I/R-induced apoptosis in RGCs. RGCs were transfected with 50 nmol/L lncRNA Ttc3-209 siRNA or scramble and then treated with or without I/R damage (ischemia for 2 hours, followed by reperfusion for 2 hours). (**A**) Real-time qPCR analysis of the expression of lncRNA Ttc3-209. (**B**) Western blotting analysis of caspase-3 and cleaved caspase-3. (**C**, **D**) Densitometric measurement of Western blotting bands for caspase-3 (**C**) and cleaved caspase-3 (**D**). (**E**, **F**) Flow cytometry analysis of total cell apoptosis. The cells in the Q1 region represent necrotic cells, the cells in the Q2 region represent late apoptotic cells, the cells in the Q3 region represent early apoptotic cells, and the cells in the Q4 region represent normal cells. Data are expressed as mean ± SD ($n = 5$). $^{\#}P < 0.05$, scramble with I/R group or lncRNA Ttc3-209 siRNA group versus scramble group; $^{*}P < 0.05$, lncRNA Ttc3-209 siRNA with I/R group versus scramble with I/R group.

Investigative Ophthalmology & Visual Science

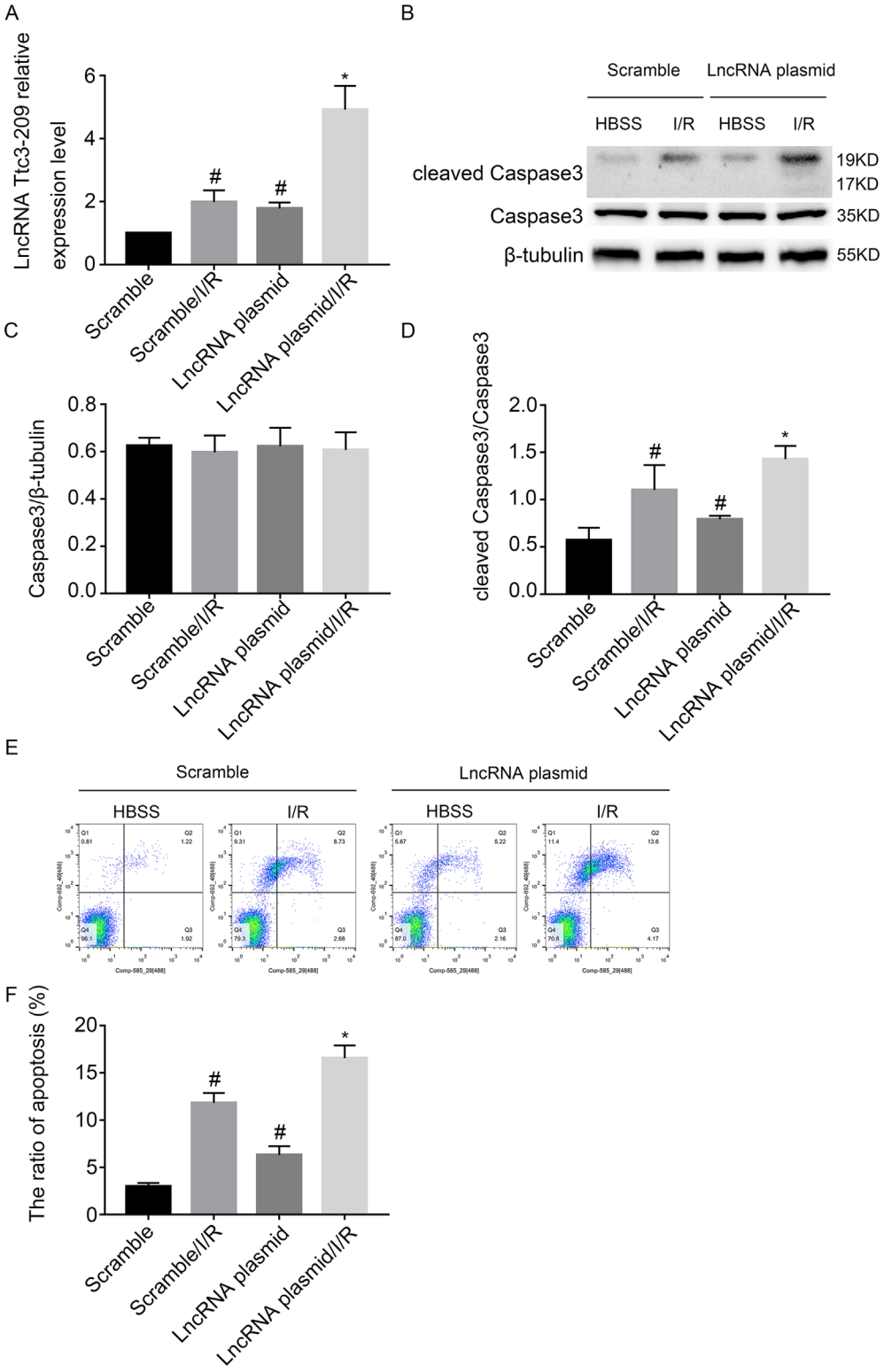

Figure 3. The overexpression of lncRNA Ttc3-209 aggravated I/R-induced apoptosis in RGCs. RGCs were transfected with 1 g/mL lncRNA Ttc3-209 plasmid or scramble and then treated with or without I/R damage. (**A**) Real-time qPCR analysis of the expression of lncRNA Ttc3-209. (**B**) Western blotting analysis of caspase-3 and cleaved caspase-3. (**C**, **D**) Densitometric measurement of Western blotting bands for caspase-3 (**C**) and cleaved caspase-3 (**D**). (**E**, **F**) Flow cytometry analysis of total cell apoptosis. The cells in the Q1 region represent necrotic cells, the cells in the Q2 region represent late apoptotic cells, the cells in the Q3 region represent early apoptotic cells, and the cells in the Q4 region represent normal cells. Data are expressed as mean ± SD ($n = 5$). $^{\#}P < 0.05$, scramble with I/R group or lncRNA Ttc3-209 group versus scramble group; $^{*}P < 0.05$, lncRNA Ttc3-209 with I/R group versus scramble with I/R group.

Investigative Ophthalmology & Visual Science

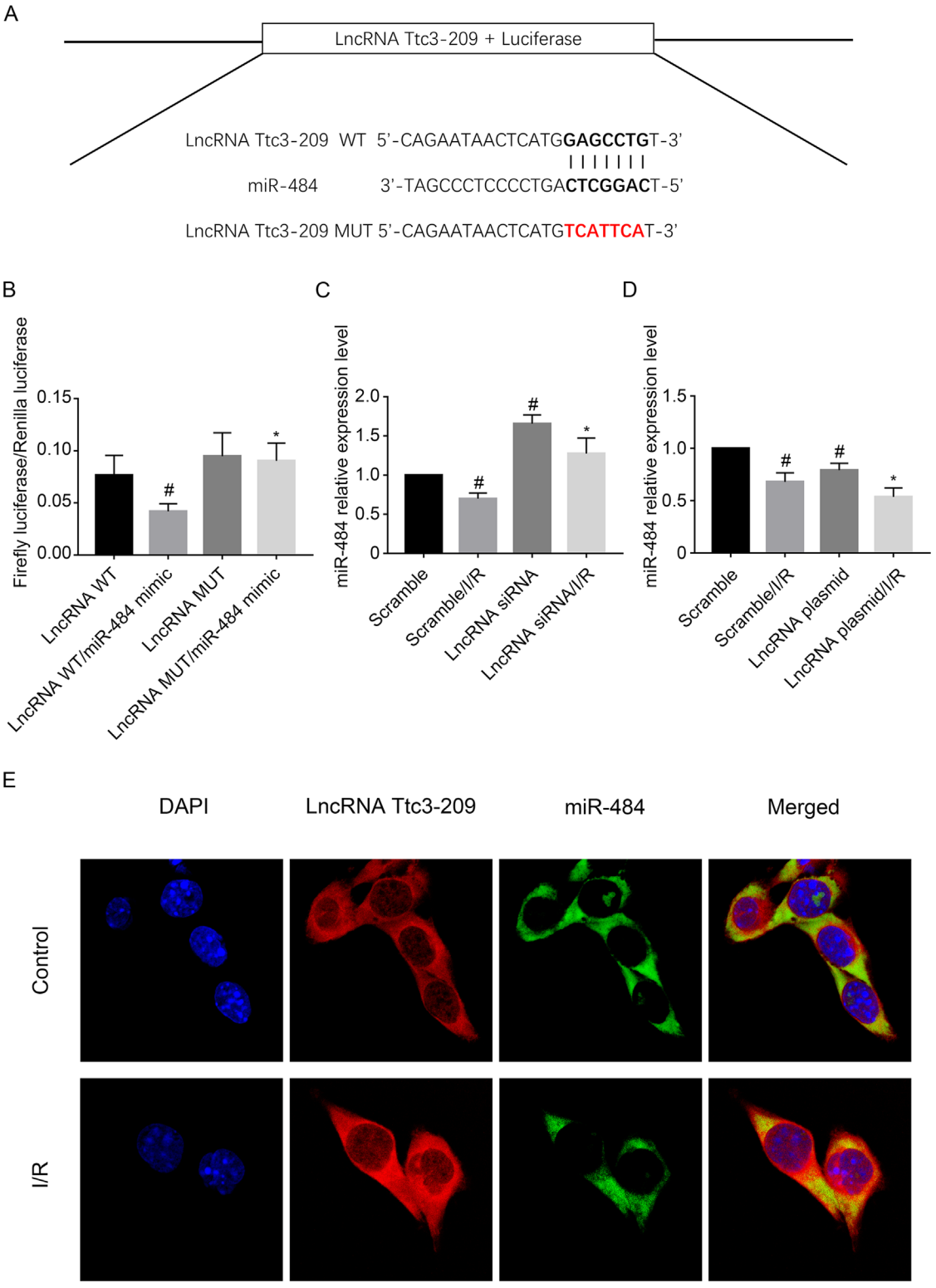

Figure 4. lncRNA Ttc3-209 bound directly to miR-484. (**A**) Sequence alignment analysis revealed that lncRNA Ttc3-209 contains the complementary sequence for miR-484. (**B**) The detection of luciferase activities after cotransfection with lncRNA Ttc3-209 WT or lncRNA Ttc3-209 MUT and miR-484 mimic or scramble. (**C**, **D**) RGCs were transfected with 50 nmol/L lncRNA Ttc3-209 siRNA or 1 g/mL lncRNA Ttc3-209 plasmid or scramble and then treated with or without I/R damage. Real-time qPCR analysis of miR-484 expression. (**E**) The intracellular colocalization of lncRNA Ttc3-209 and miR-484 in RGCs with or without I/R treatment. *Scale bar*: 10 µm. Data are expressed as mean ± SD ($n = 5$). $^{\#}P < 0.05$, scramble with I/R group or lncRNA Ttc3-209 siRNA group or lncRNA Ttc3-209 group versus scramble group, lncRNA Ttc3-209 WT/miR-484 mimic group versus lncRNA Ttc3-209 WT group; $^{*}P < 0.05$, lncRNA Ttc3-209 siRNA with I/R group or lncRNA Ttc3-209 with I/R group versus scramble with I/R group, lncRNA Ttc3-209 MUT/miR-484 mimic group versus lncRNA Ttc3-209 WT/miR-484 mimic group.

Investigative Ophthalmology & Visual Science

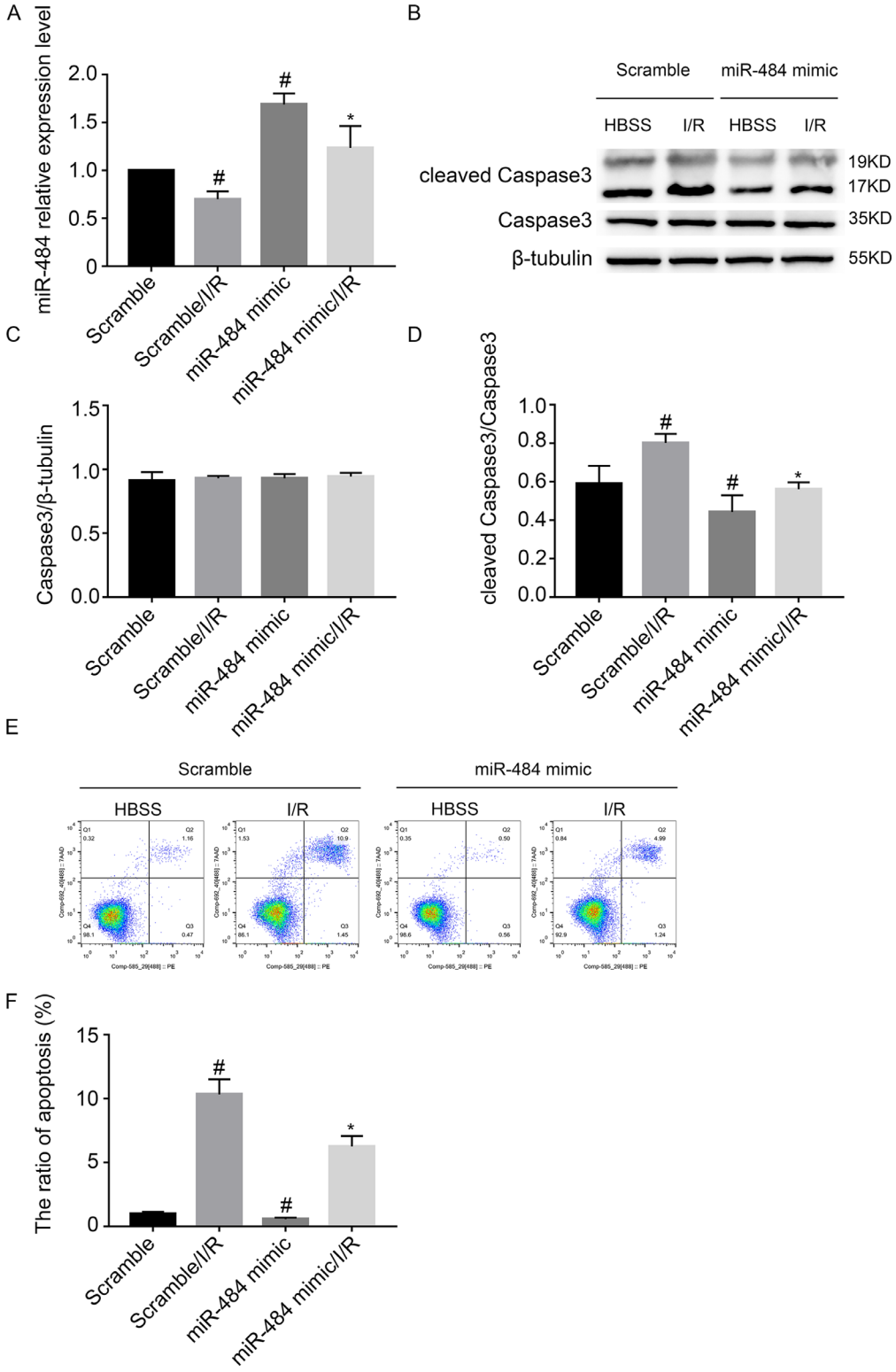

Figure 5. The overexpression of miR-484 ameliorated I/R-induced apoptosis in RGCs. RGCs were transfected with 50 nmol/L miR-484 mimic or scramble and then treated with or without I/R damage. (**A**) Real-time qPCR analysis of miR-484 expression. (**B**) Western blotting analysis of caspase-3 and cleaved caspase-3. (**C**, **D**) Densitometric measurement of Western blotting bands for caspase-3 (**C**) and cleaved caspase-3 (**D**). (**E**, **F**) Flow cytometry analysis of total cell apoptosis. The cells in the Q1 region represent necrotic cells, the cells in the Q2 region represent late apoptotic cells, the cells in the Q3 region represent early apoptotic cells, and the cells in the Q4 region represent normal cells. Data are expressed as mean ± SD ($n = 5$). $^{\#}P < 0.05$, scramble with I/R group or miR-484 mimic group versus scramble group; $^{*}P < 0.05$, miR-484 mimic with I/R group versus scramble with I/R group.

Investigative Ophthalmology & Visual Science

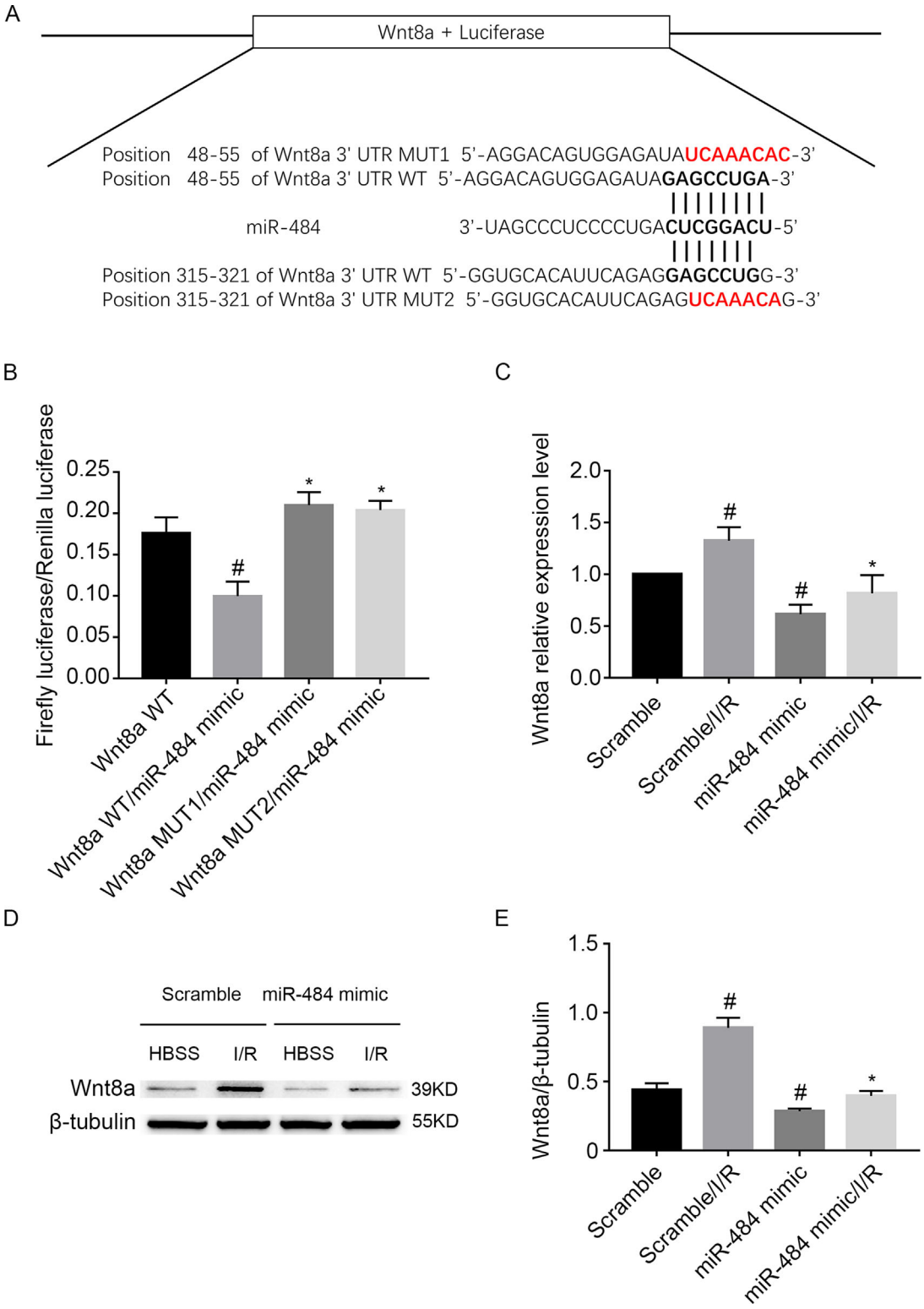

Figure 6. Wnt8a was identified as a target gene for miR-484. RGCs were transfected with 50 nmol/L miR-484 mimic or scramble and then treated with or without I/R damage. (**A**) Putative miR-484 complementary binding sites in the 3′-UTR of mouse Wnt8a mRNA. (**B**) Detection of luciferase activities after cotransfection with the 3′-UTR luciferase reporter vectors for mouse Wnt8a-WT, Wnt8a-MUT1, Wnt8a-MUT2, miR-484 mimic, or scramble. (**C**) Real-time qPCR analysis of Wnt8a mRNA expression. (**D**, **E**) Western blotting analysis of Wnt8a (**D**) and densitometric measurement of Western blotting bands (**E**). Data are expressed as mean ± SD ($n = 5$). $^{\#}P < 0.05$, Wnt8a-WT/miR-484 mimic group versus Wnt8a-WT group, scramble with I/R group or miR-484 mimic group versus scramble group; $^{*}P < 0.05$, Wnt8a-MUT1/miR-484 mimic group or Wnt8a-MUT2/miR-484 mimic group versus Wnt8a-WT/miR-484 mimic group, miR-484 mimic with I/R group versus scramble with I/R group.

Investigative Ophthalmology & Visual Science

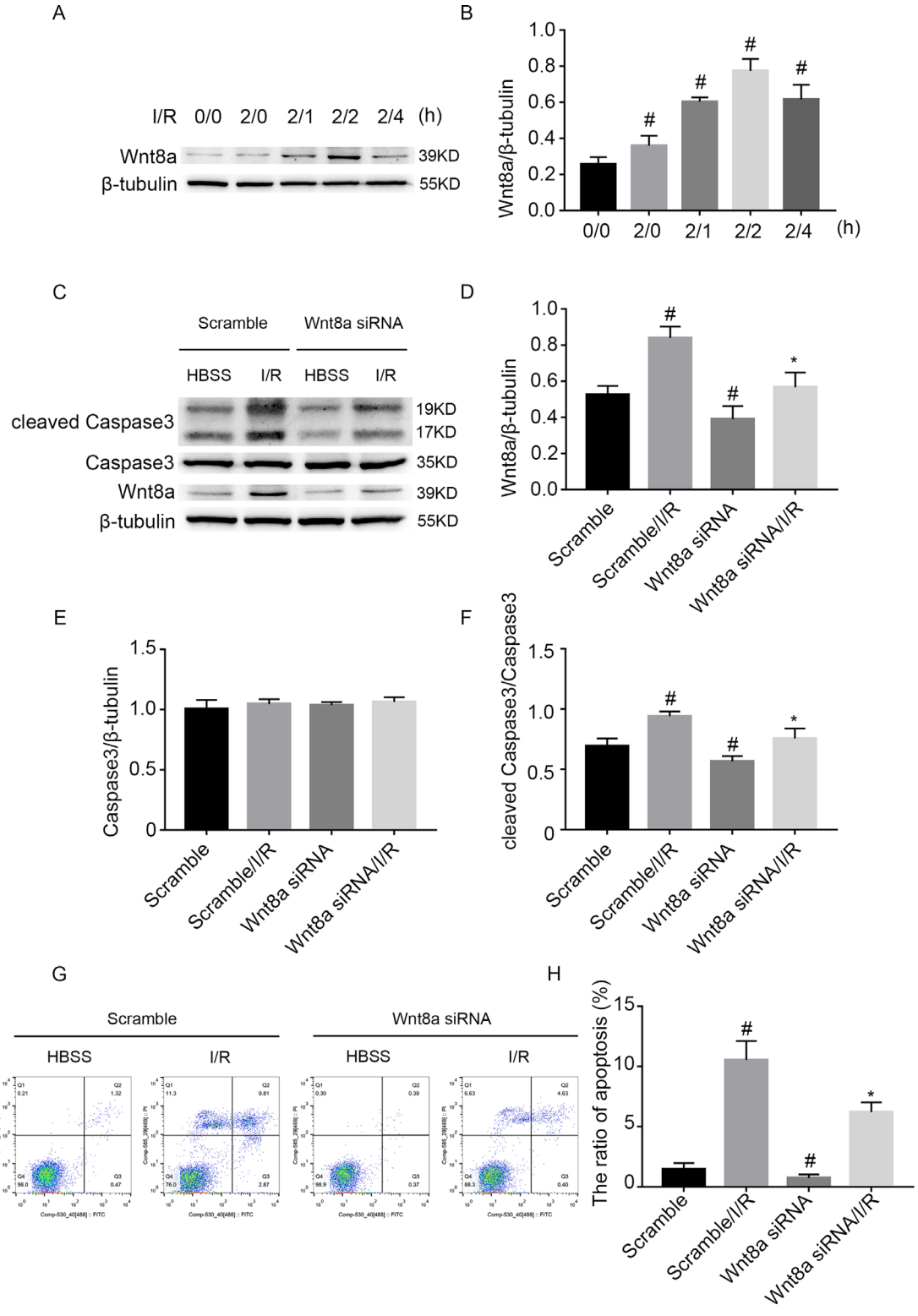

Figure 7. Wnt8a knockdown suppressed the I/R-induced RGC apoptosis. RGCs were transfected with 50 nmol/L Wnt8a siRNA or scramble and then treated with or without I/R damage. (**A**) RGCs were treated with or without I/R at indicated time points (I/R for 0/0, 2/0, 2/1, 2/2, 2/4 hours, respectively). The expression levels of Wnt8a were detected by Western blot. (**B**) Densitometric measurement of Western blot bands for Wnt8a. (**C**) Western Blot analysis of Wnt8a, caspase-3, and cleaved caspase-3. (**D–F**) Densitometric measurement of Western blot bands for Wnt8a, caspase-3, and cleaved caspase-3. (**G**, **H**) Flow cytometry analysis of total cell apoptosis. The cells in the Q1 region represent necrotic cells, the cells in the Q2 region represent late apoptotic cells, the cells in the Q3 region represent early apoptotic cells, and the cells in the Q4 region represent normal cells. Data are expressed as mean ± SD ($n = 5$). $^{\#}P < 0.05$, I/R for 2/0, 2/1, 2/2, 2/4 hours, respectively, versus 0/0 hour, scramble with I/R group or Wnt8a siRNA group versus scramble group; $^{*}P < 0.05$, Wnt8a siRNA with I/R group versus scramble with I/R group.

Investigative Ophthalmology & Visual Science

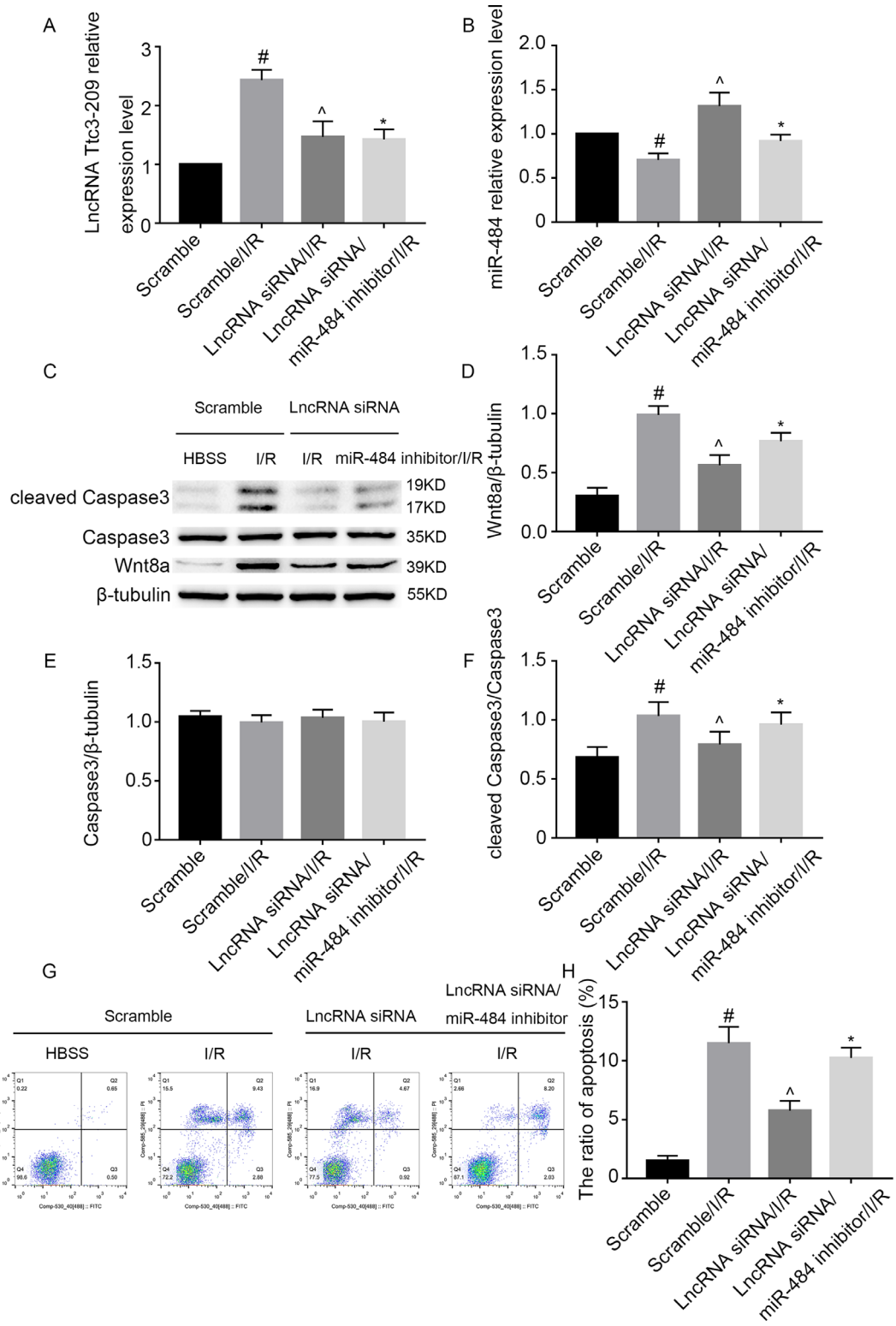

Figure 8. Inhibition of lncRNA Ttc3-209 alleviated the I/R-induced RGC apoptosis, which was reversed by the inhibitor of miR-484. RGCs were cotransfected with lncRNA Ttc3-209 siRNA (50 nmol/L) and miR-484 inhibitor (50 nmol/L) or scramble and then treated with or without I/R damage. (**A**, **B**) Real-time qPCR analysis of lncRNA Ttc3-209 expression (**A**) and miR-484 (**B**). (**C–F**) Western blot analysis of Wnt8a, caspase-3, and cleaved caspase-3 (**C**) and densitometric measurement of Western blot bands (**D–F**). (**G**, **H**) Flow cytometry analysis of total cell apoptosis. The cells in the Q1 region represent necrotic cells, the cells in the Q2 region represent late apoptotic cells, the cells in the Q3 region represent early apoptotic cells, and the cells in the Q4 region represent normal cells. Data are expressed as mean ± SD ($n = 5$). $^{\#}P < 0.05$, scramble with I/R group versus scramble group; $^{\wedge}P < 0.05$, lncRNA Ttc3-209 siRNA with I/R group versus scramble with I/R group; $^{*}P < 0.05$, lncRNA Ttc3-209 siRNA/miR-484 inhibitor with I/R group versus lncRNA Ttc3-209 siRNA with I/R group.

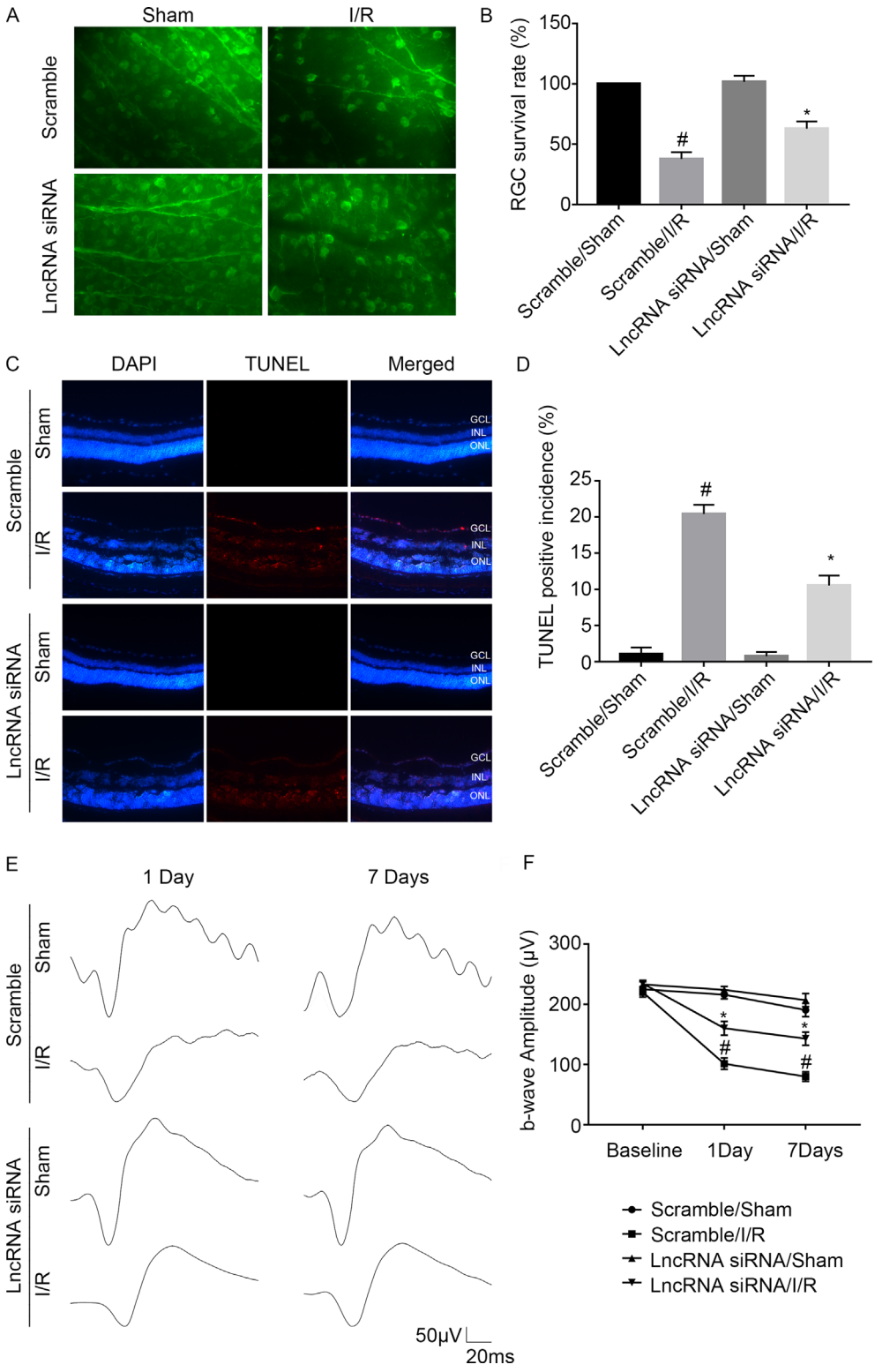

Figure 9. Suppression of lncRNA Ttc3-209 mitigated I/R-induced apoptosis in RGCs and improved the visual function of C57BL/6J mice. C57BL/6J mice were preinjected with 1 μL (1 μg/μL) lncRNA Ttc3-209 siRNA or scramble into the vitreous chamber for 24 hours. Next, the intraocular pressure was elevated to 120 mm Hg for 1 hour and then changed to reperfusion for 24 hours. (**A**, **B**) Seven days after ischemia injury, the retinas were removed for Tuj1 immunofluorescence staining. Representative images (**A**) of each group to visualize the surviving retinal ganglion cells along with statistical analysis (**B**) as normalized by the scramble/sham group. *Scale bar*: 50 μm. (**C**, **D**) Representative TUNEL staining images (**C**) of frozen retinal sections after 24 hours of reperfusion and relevant statistical analysis (**D**) as normalized by the total number of nuclei in the ganglion cell layer of each image. *Scale bar*: 100 μm. (**E**, **F**) Representative scotopic ERG (**E**) in vivo with an intensity of 3.0 cds/m^2 at baseline, 1 day, and 7 days after retinal ischemia and relevant statistical analysis (**F**) of b-wave amplitudes. Data are expressed as mean ± SD ($n = 5$). $^{\#}P < 0.05$, scramble/I/R group versus scramble/sham group; $^{*}P < 0.05$, lncRNA Ttc3-209 siRNA/I/R group versus scramble/I/R group.

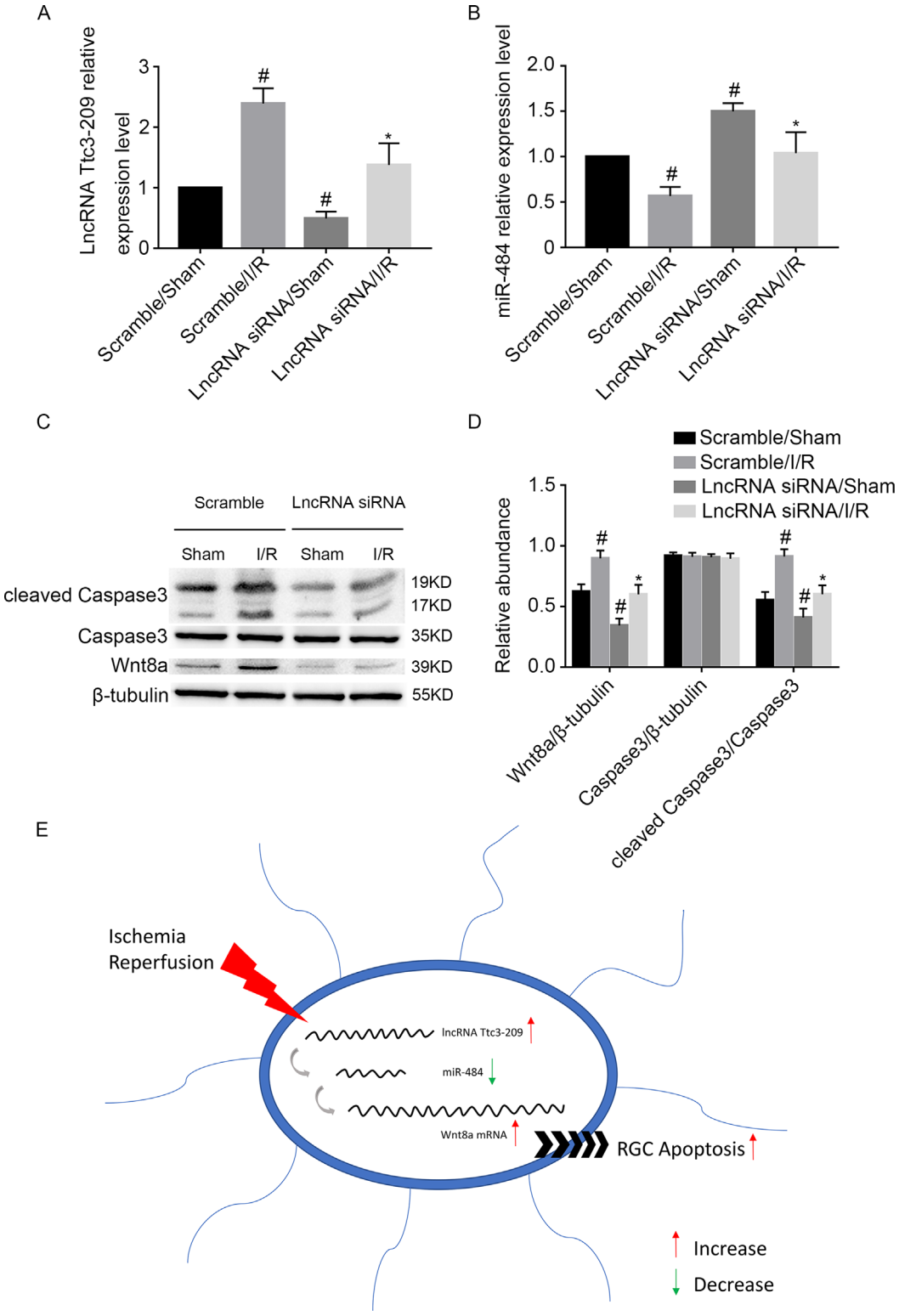

Figure 10. The downregulation of lncRNA Ttc3-209 diminished I/R-induced apoptosis in RGC apoptosis via the lncRNA Ttc3-209/miR-484/Wnt8a axis in C57BL/6J mice. C57BL/6J mice were preinjected with 1 µL (1 µg/µL) lncRNA Ttc3-209 siRNA or scramble into the vitreous chamber for 24 hours. Next, the intraocular pressure was elevated to 120 mm Hg for 1 hour and then changed to reperfusion for 24 hours. Finally, the retinal tissue was removed to conduct a series of experiments. (**A**) Real-time qPCR analysis of the expression of lncRNA Ttc3-209. (**B**) Real-time qPCR analysis of miR-484 expression. (**C**, **D**) Western blotting analysis of Wnt8a, caspase-3, and cleaved caspase-3 (**C**) and the densitometric measurement of Western blotting bands (**D**). (**E**) The role and molecular mechanism that regulates the effects of lncRNA Ttc3-209 in the I/R-induced apoptosis of RGCs. Data are expressed as mean ± SD ($n = 5$). $^{\#}P < 0.05$, scramble/I/R group or lncRNA Ttc3-209 siRNA/sham group versus scramble/sham group; $^{*}P < 0.05$, lncRNA Ttc3-209/I/R group versus scramble/I/R group.

Investigative Ophthalmology & Visual Science

blotting findings and confirmed the existence of a potential apoptosis-related mechanism (Figs. 8G, 8H).

The Suppression of lncRNA Ttc3-209 Mitigated I/R-Induced Apoptosis in RGCs and Improved the Visual Function of C57BL/6J Mice

We also created animal models to illustrate the effect of lncRNA Ttc3-209 on I/R-induced apoptosis in RGCs in vivo. The immunostaining of Tuj1 (neuronal class III β-tubulin) in a stretched preparation of retina showed that a preoperative injection of lncRNA Ttc3-209 into the vitreous chamber significantly improved the number of surviving retinal ganglion cells following RIR injury (Figs. 9A, 9B). Furthermore, the TUNEL staining of frozen retinal sections indicated that there were notably fewer apoptotic cells in the ganglion cell layer when comparing the lncRNA Ttc3-209 siRNA/I/R group with the scramble/I/R group (Figs. 9C, 9D). We also performed scotopic ERG examinations to evaluate the visual function of mice before and after I/R injury. With increased time after injury, we noticed a decline in the b-wave amplitudes of all mice. However, mice treated with lncRNA Ttc3-209 siRNA/I/R exhibited a significantly slower decline than the scramble/I/R mice (Figs. 9E, 9F).

The Downregulation of lncRNA Ttc3-209 Diminished I/R-Induced Apoptosis in RGCs via the lncRNA Ttc3-209/miR-484/Wnt8a Axis in C57BL/6J Mice

We also investigated the molecular mechanisms underlying apoptosis in RGCs using animal models. First, we investigated the knockdown efficiency of lncRNA Ttc3-209 siRNA knockdown by real-time qPCR (Fig. 10A). Real-time qPCR showed that lncRNA Ttc3-209 knockdown relieved the I/R-induced suppression of miR-484 (Fig. 10B). Finally, Western blotting analysis suggested that lncRNA Ttc3-209 siRNA markedly reduced the I/R-induced expression of cleaved caspase-3 and Wnt8a (Figs. 10C, 10D). In summary, these data revealed that the knockdown of lncRNA Ttc3-209 diminished I/R-induced apoptosis in RGCs in C57BL/6J mice via the lncRNA Ttc3-209/miR-484/Wnt8a axis (Fig. 10E).

Discussion

Healthy RGCs are of vital importance to normal visual function. Over the past few decades, the death of RGCs induced by retinal ischemia reperfusion has been recognized as the main factor responsible for the irreversible impairment of visual function.[4] As a consequence, protecting RGCs from injury is a focal point of therapy for retinal ischemia reperfusion. Numerous studies have reported that lncRNAs participate in the pathogenesis of various ophthalmic diseases and regulate gene expression at the pretranscriptional, transcriptional, and posttranscriptional levels.[5] The findings of a recent study indicated that methyl-CpG binding domain protein 2 (Mbd2) mediates retinal cell apoptosis via the lncRNA Mbd2-AL1/miR-188-3p/Traf3 signaling pathway in ischemia reperfusion injury.[17] In our present study, we demonstrated, for the first time, that lncRNA Ttc3-209 was induced by I/R damage in RGCs. In addition, lncRNA Ttc3-209 was found to mediate I/R-induced apoptosis in RGCs. Therefore, lncRNA Ttc3-209 may represent a new target for the treatment of retinal ischemia reperfusion.

Numerous studies have suggested that lncRNAs play an important role in I/R injury.[30–34] Nevertheless, only some of these lncRNAs are involved in the regulation of cell apoptosis. For example, lncRNA C2dat1 is known to regulate calcium/calmodulin-dependent kinase II δ expression to promote neuronal survival via the nuclear factor–κB signaling pathway following cerebral ischemia.[35] lncRNA H19 is known to initiate microglial pyroptosis and neuronal death following retinal I/R injury.[36] Furthermore, PM2.5 exposure aggravated myocardial I/R injury lncRNA (PEAMIR) was found to inhibit apoptosis and the inflammatory response in PM2.5-exposed aggravated myocardial ischemia/reperfusion injury as a ceRNA of miR-29b-3p.[37] In our current study, we used lncRNA chip analysis to show that lncRNA Ttc3-209, located in the cytoplasm of RGCs, was significantly induced by I/R; this was further confirmed by real-time qPCR (Fig. 1). In addition, I/R-induced apoptosis was enhanced in RGCs by the overexpression of lncRNA Ttc3-209 (Fig. 3) but was attenuated by its knockdown (Fig. 2). Similar findings were observed in vivo in that lncRNA Ttc3-209 siRNA ameliorated the I/R-induced apoptosis of RGCs from C57BL/6J mice, thus leading to an improvement in visual function (Figs. 9, 10A, 10C, 10D). Collectively, these data showed that the application of endogenous lncRNA Ttc3-209 exerts a proapoptotic effect.

An increasing number of studies have demonstrated that lncRNAs act as ceRNAs to sponge miRNAs and then regulate the expression of target genes.[13,38–40] For instance, lncRNA LINC01234 functions as a ceRNA to mediate core-binding factor β (CBFB) expression by sponging miR-204-5p in gastric cancer.[41] lncRNA AK038897 is also known to aggravate cerebral I/R injury by acting as a ceRNA for miR-26a-5p to target DAPK1.[42] By using RegRNA software (http://regrna2.mbc.nctu.edu.tw/), we focused on miR-484 as the putative target of lncRNA Ttc3-209. A series of subsequent experiments provided strong evidence to support this prediction. Following I/R, the suppression of miR-484 was enhanced by the overexpression of lncRNA Ttc3-209 (Fig. 4D); this effect was reversed by lncRNA Ttc3-209 siRNA (Fig. 4C). Second, dual-luciferase reporter assays indicated that lncRNA Ttc3-209 bound directly to miR-484 (Figs. 4A, 4B). Finally, FISH colocalization assays further revealed the interaction between lncRNA Ttc3-209 and miR-484 (Fig. 4E). However, the role of miR-484 during the process of apoptosis in RGCs remains largely obscure. A number of studies support the antiapoptotic function of miR-484 in a variety of cells.[18,43–47] However, another previous study reported that the suppression of lncRNA H19 significantly reduced the viability of A549 cell viability, migration, and invasion but promoted apoptosis by targeting miR-484 in human lung cancer cells.[48] In this study, we found that the overexpression of miR-484 attenuated the apoptosis of RGCs induced by I/R damage; this opposed the effects arising from lncRNA Ttc3-209 treatment (Fig. 5). Collectively, these data suggest that miR-484 is a direct target of lncRNA Ttc3-209 and alleviates I/R-induced apoptosis in RGCs.

In order to determine the mechanisms underlying the antiapoptotic effect of miR-484, we predicted the target gene for miR-484 by using TargetScanMouse 7.2 software; our analysis identified Wnt8a as a putative target. It has been reported that the chromatin remodeling protein Bptf promotes posterior neuroectodermal fate by enhancing Smad2-activated Wnt8a expression.[49] Another study also indicated that the activation of peroxisome proliferator-activated receptor α by clofibrate sensitizes pancreatic

Investigative Ophthalmology & Visual Science

cancer cells to radiation via the Wnt8a/β-catenin pathway.[50] We then carried out several experiments to demonstrate our hypothesis that miR-484 targets Wnt8a. First, at the transcriptional and translational levels, the overexpression of miR-484 inhibited the expression of Wnt8a mRNA and protein induced by I/R treatment (Figs. 6C–E). Second, dual-luciferase reporter assays indicated that miR-484 bound to the 3′-UTR of Wnt8a (Figs. 6A, 6B). A previous review stated that WNT signaling molecules play key roles during embryogenesis, tissue regeneration, and carcinogenesis.[51] However, only a few studies have reported that Wnt8a is able to interact closely with apoptosis.[19,50,52–55] To elucidate how Wnt8a affected I/R-induced apoptosis in RGCs, we transfected RGCs with Wnt8a siRNA. Results showed that Wnt8a was induced by I/R treatment in RGCs (Figs. 7A, 7B) and that the knockdown of Wnt8a reduced apoptosis in RGCs following I/R (Figs. 7C–H). Moreover, we verified that the knockdown of lncRNA Ttc3-209 reduced I/R-induced apoptosis in RGCs via the upregulation of miR484 and then downregulation of Wnt8a; this was reversed by a miR484 inhibitor (Fig. 8). All of these molecular changes were confirmed in vivo and visual function improved significantly when suppressing lncRNA Ttc3-209 in C57BL/6J mice (Figs. 9, 10A, 10D). Overall, these data imply that miR-484 decoys Wnt8a by combining with its 3′-UTR and that Wnt8a is an inducer of apoptosis. Our data indicate that lncRNA Ttc3-209 mediates I/R-induced apoptosis in RGCs via the lncRNA Ttc3-209/miR-484/Wnt8a axis (Fig. 10E).

In summary, our study demonstrates that I/R damage induces the expression of lncRNA Ttc3-209 in RGCs and that lncRNA Ttc3-209 promotes the apoptosis of RGCs following injury. Mechanistically, lncRNA Ttc3-209 acts as a ceRNA competing for and sponging miR-484. This reduces the combination of miR484 and Wnt8a 3′-UTR and increases the expression of Wnt8a, thus aggravating I/R-induced apoptosis in RGCs. Hence, lncRNA Ttc3-209 might provide a novel insight into the pathogenesis and treatment of retinal ischemia reperfusion.

Acknowledgments

The authors thank EditSprings for the expert linguistic services provided.

Supported by the National Natural Science Foundation of China (Reference: 81770951), the Natural Science Foundation of Hunan Province (Reference: 2018JJ3742), and the Fundamental Research Funds for the Central Universities of Central South University (2020zzts878).

Disclosure: **R. Zhang**, None; **Y. Feng**, None; **J. Lu**, None; **Y. Ge**, None; **H. Li**, None

References

1. Russo R, Berliocchi L, Adornetto A, et al. Calpain-mediated cleavage of Beclin-1 and autophagy deregulation following retinal ischemic injury in vivo. *Cell Death Dis*. 2011;2(4):e144.
2. Osborne NN, Schmidt KG. Neuroprotection against glaucoma remains a concept [in German]. *Ophthalmologe*. 2004;101(11):1087–1092.
3. Dvoriantchikova G, Degterev A, Ivanov D. Retinal ganglion cell (RGC) programmed necrosis contributes to ischemia-reperfusion-induced retinal damage. *Exp Eye Res*. 2014;123:1–7.
4. Almasieh M, Wilson A M, Morquette B, et al. The molecular basis of retinal ganglion cell death in glaucoma. *Prog Retinal Eye Res*. 2012;31(2):152–181.
5. Zhang L, Dong Y, Wang Y, et al. Long non-coding RNAs in ocular diseases: new and potential therapeutic targets. *FEBS J*. 2019;286(12):2261–2272.
6. Chen M, Wu X, Ma W, et al. Decreased expression of lncRNA VPS9D1-AS1 in gastric cancer and its clinical significance. *Cancer Biomark*. 2017;21(1):23–28.
7. Li J, Li Z, Zheng W, et al. lncRNA-ATB: an indispensable cancer-related long noncoding RNA. *Cell Prolif*. 2017;50(6):e12381.
8. Liu Y, Sun Z, Zhu J, et al. lncRNA-TCONS_00034812 in cell proliferation and apoptosis of pulmonary artery smooth muscle cells and its mechanism. *J Cell Physiol*. 2018;233(6):4801–4814.
9. Zhang ZK, Li J, Guan D, et al. A newly identified lncRNA MAR1 acts as a miR-487b sponge to promote skeletal muscle differentiation and regeneration. *J Cachexia Sarcopenia Muscle*. 2018;9(3):613–626.
10. Zhao L, Kong H, Sun H, et al. lncRNA-PVT1 promotes pancreatic cancer cells proliferation and migration through acting as a molecular sponge to regulate miR-448. *J Cell Physiol*. 2018;233(5):4044–4055.
11. Liu Y, Yang Y, Li L, et al. lncRNA SNHG1 enhances cell proliferation, migration, and invasion in cervical cancer. *Biochem Cell Biol*. 2018;96(1):38–43.
12. Ma Y, Yang Y, Wang F, et al. Long non-coding RNA CCAL regulates colorectal cancer progression by activating Wnt/β-catenin signalling pathway via suppression of activator protein 2α. *Gut*. 2016;65(9):1494–1504.
13. Liu H, Xu D, Zhong X, et al. lncRNA-mRNA competing endogenous RNA network depicts transcriptional regulation in ischaemia reperfusion injury. *J Cell Mol Med*. 2019;23(3):2272–2276.
14. Zhang G, Li S, Lu J, et al. lncRNA MT1JP functions as a ceRNA in regulating FBXW7 through competitively binding to miR-92a-3p in gastric cancer. *Mol Cancer*. 2018;17(1):87.
15. Platania CBM, Maisto R, Trotta MC, et al. Retinal and circulating miRNA expression patterns in diabetic retinopathy: an in silico and in vivo approach. *Br J Pharmacol*. 2019;176(13):2179–2194.
16. Romano GL, Platania CB, Forte S, et al. MicroRNA target prediction in glaucoma. *Prog Brain Res*. 2015;220:217–240.
17. Ge Y, Zhang R, Feng Y, et al. Mbd2 mediates retinal cell apoptosis by targeting the lncRNA Mbd2-AL1/miR-188-3p/Traf3 axis in ischemia/reperfusion injury. *Mol Ther Nucleic Acids*. 2020:19:1250–1265.
18. Wang K, Long B, Jiao JQ, et al. miR-484 regulates mitochondrial network through targeting Fis1. *Nat Commun*. 2012;3:781.
19. Brock CK, Wallin ST, Ruiz OE, et al. Stem cell proliferation is induced by apoptotic bodies from dying cells during epithelial tissue maintenance. *Nat Commun*. 2019;10(1):1044.
20. Yao J, Wang XQ, Li YJ, et al. Long non-coding RNA MALAT1 regulates retinal neurodegeneration through CREB signaling. *EMBO Mol Med*. 2016;8(4):346–362.
21. Barres BA, Silverstein BE, Corey DP, et al. Immunological, morphological, and electrophysiological variation among retinal ganglion cells purified by panning. *Neuron*. 1988;1(9):791–803.
22. Emala CW. Preconditioning and adenosine protect human proximal tubule cells in an in vitro model of ischemic injury. *J Am Soc Nephrol*. 2002;13(11):2753–2761.
23. Kleinman ME, Yamada K, Takeda A, et al. Sequence- and target-independent angiogenesis suppression by siRNA via TLR3. *Nature*. 2008;452(7187):591–597.
24. Zhu M, Jiang L, Yuan Y, et al. Intravitreal Ets1 siRNA alleviates choroidal neovascularization in a mouse model

of age-related macular degeneration. *Cell Tissue Res*. 2019;376(3):341–351.

25. Li H, Zhu X, Fang F, et al. Down-regulation of GRP78 enhances apoptosis via CHOP pathway in retinal ischemia-reperfusion injury. *Neurosci Lett*. 2014;575:68–73.
26. Kim, BJ, Braun TA, Wordinger RJ, et al. Progressive morphological changes and impaired retinal function associated with temporal regulation of gene expression after retinal ischemia/reperfusion injury in mice. *Mol Neurodegeneration*. 2013;8:21.
27. Mathew B, Ravindran S, Liu X, et al. Mesenchymal stem cell-derived extracellular vesicles and retinal ischemia-reperfusion. *Biomaterials*. 2019;197:146–160.
28. Russo R, Varano GP, Adornetto A, et al. Rapamycin and fasting sustain autophagy response activated by ischemia/reperfusion injury and promote retinal ganglion cell survival. *Cell Death Dis*. 2018;9(10):981.
29. Grozdanic SD, Sakaguchi DS, Kwon YH, et al. Functional characterization of retina and optic nerve after acute ocular ischemia in rats. *Invest Ophthalmol Vis Sci*. 2003;44(6):2597–2605.
30. Wang JX, Zhang XJ, Li Q, et al. MicroRNA-103/107 regulate programmed necrosis and myocardial ischemia/reperfusion injury through targeting FADD. *Circ Res*. 2015;117(4):352–363.
31. Vausort M, Wagner DR, Devaux Y. Long noncoding RNAs in patients with acute myocardial infarction. *Circ Res*. 2014;115(7):668–677.
32. Liu CY, Zhang YH, Li RB, et al. lncRNA CAIF inhibits autophagy and attenuates myocardial infarction by blocking p53-mediated myocardin transcription. *Nat Commun*. 2018;9(1):29.
33. Hardeland R. Melatonin and inflammation—story of a double-edged blade. *J Pineal Res*. 2018;65(4):e12525.
34. Boon RA, Jaé N, Holdt L, et al. Long noncoding RNAs: from clinical genetics to therapeutic targets? *J Am Coll Cardiol*. 2016;67(10):1214–1226.
35. Xu Q, Deng F, Xing Z, et al. Long non-coding RNA C2dat1 regulates CaMKIIδ expression to promote neuronal survival through the NF-κB signaling pathway following cerebral ischemia. *Cell Death Dis*. 2016;7(3):e2173.
36. Wan P, Su W, Zhang Y, et al. lncRNA H19 initiates microglial pyroptosis and neuronal death in retinal ischemia/reperfusion injury. *Cell Death Differentiation*. 2020;27(1):176–191.
37. Pei YH, Chen J, Wu X, et al. lncRNA PEAMIR inhibits apoptosis and inflammatory response in PM2.5 exposure aggravated myocardial ischemia/reperfusion injury as a competing endogenous RNA of miR-29b-3p. *Nanotoxicology*. 2020;14(5):638–653.
38. Tay Y, Rinn J, Pandolfi PP. The multilayered complexity of ceRNA crosstalk and competition. *Nature*. 2014;505(7483):344–352.
39. Yamamura S, Imai-Sumida M, Tanaka Y, et al. Interaction and cross-talk between non-coding RNAs. *Cell Mol Life Sci*. 2018;75(3):467–484.
40. Rashid F, Shah A, Shan G. Long non-coding RNAs in the cytoplasm. *Genomics Proteomics Bioinformatics*. 2016;14(2):73–80.
41. Chen X, Chen Z, Yu S, et al. Long noncoding RNA LINC01234 functions as a competing endogenous RNA to regulate CBFB expression by sponging miR-204-5p in gastric cancer. *Clin Cancer Res*. 2018;24(8):2002–2014.
42. Wei R, Zhang L, Hu W, et al. Long non-coding RNA AK038897 aggravates cerebral ischemia/reperfusion injury via acting as a ceRNA for miR-26a-5p to target DAPK1. *Exp Neurol*. 2019;314:100–110.
43. Vasyutina E, Boucas JM, Bloehdorn J, et al. The regulatory interaction of EVI1 with the TCL1A oncogene impacts cell survival and clinical outcome in CLL. *Leukemia*. 2015;29(10):2003–2014.
44. Vijayarathna S, Sasidharan S. Functional validation of downregulated microRNAs in HeLa Cells treated with *Polyalthia longifolia* leaf extract using different microscopic approaches: a morphological alteration-based validation. *Microsc Microanal*. 2019;25(5):1263–1272.
45. Liu H, Li S, Jiang W, et al. MiR-484 protects rat myocardial cells from ischemia-reperfusion injury by inhibiting caspase-3 and caspase-9 during apoptosis. *Korean Circ J*. 2020;50(3):250–263.
46. Li J, Li L, Li X, et al. Long noncoding RNA LINC00339 aggravates doxorubicin-induced cardiomyocyte apoptosis by targeting miR-484. *Biochem Biophys Res Commun*. 2018;503(4):3038–3043.
47. Hu Y, Xie H, Liu Y, et al. miR-484 suppresses proliferation and epithelial-mesenchymal transition by targeting ZEB1 and SMAD2 in cervical cancer cells. *Cancer Cell Int*. 2017;17:36.
48. Zhang Q, Li X, Li X, et al. lncRNA H19 promotes epithelial-mesenchymal transition (EMT) by targeting miR-484 in human lung cancer cells. *J Cell Biochem*. 2018;119(6):4447–4457.
49. Ma Y, Liu X, Liu Z, et al. The chromatin remodeling protein Bptf promotes posterior neuroectodermal fate by enhancing Smad2-activated wnt8a expression. *J Neurosci*. 2015;35(22):8493–8506.
50. Xue J, Zhu W, Song J, et al. Activation of PPARα by clofibrate sensitizes pancreatic cancer cells to radiation through the Wnt/β-catenin pathway. *Oncogene*. 2018;37(7):953–962.
51. Katoh M. Networking of WNT, FGF, Notch, BMP, and Hedgehog signaling pathways during carcinogenesis. *Stem Cell Rev*. 2007;3(1):30–38.
52. Niederreither K, Vermot J, Schuhbaur B, et al. Retinoic acid synthesis and hindbrain patterning in the mouse embryo. *Development (Cambridge, England)*. 2000;127(1):75–85.
53. Mahoney Rogers AA, Zhang J, Shim K. Sprouty1 and Sprouty2 limit both the size of the otic placode and hindbrain Wnt8a by antagonizing FGF signaling. *Dev Biol*. 2011;353(1):94–104.
54. Naylor RW, Han HI, Hukriede NA, et al. Wnt8a expands the pool of embryonic kidney progenitors in zebrafish. *Dev Biol*. 2017;425(2):130–141.
55. Li J, Zhang Y, Liu K, et al. Xiaoaiping induces developmental toxicity in zebrafish embryos through activation of ER stress, apoptosis and the Wnt pathway. *Front Pharmacol*. 2018;9:1250.

Investigative Ophthalmology & Visual Science